

Vratislava Mořová

Integral transforms – the base of recent technologies

In: Jan Brandts and Sergey Korotov and Michal Křížek and Jakub Šístek and Tomáš Vejchodský (eds.): Applications of Mathematics 2013, In honor of the 70th birthday of Karel Segeth, Proceedings. Prague, May 15-17, 2013. Institute of Mathematics AS CR, Prague, 2013. pp. 158–167.

Persistent URL: <http://dml.cz/dmlcz/702942>

Terms of use:

© Institute of Mathematics AS CR, 2013

Institute of Mathematics of the Czech Academy of Sciences provides access to digitized documents strictly for personal use. Each copy of any part of this document must contain these *Terms of use*.



This document has been digitized, optimized for electronic delivery and stamped with digital signature within the project *DML-CZ: The Czech Digital Mathematics Library*
<http://dml.cz>

INTEGRAL TRANSFORMS – THE BASE OF RECENT TECHNOLOGIES

Vratislava Mošová

Moravian University College Olomouc
Jeremenkova 1142/42, 772 00 Olomouc, Czech Republic
vratislava.mosova@mvso.cz

Abstract

In this article, the attention is paid to Fourier, wavelet and Radon transforms. A short description of them is given. Their application in signal processing especially for repairing sound and reconstructing image is outlined together with several simple examples.

1. Introduction

In this survey paper we will deal with such integral transforms that are used in the image or sound processing. The transforms, we will speak about, were defined already long time ago. Joseph Fourier approximated 2π periodic functions by trigonometric series in 1778. The first wavelet basis – Haar wavelets – was proposed as an example of a countable orthonormal system in $L^2(\mathbb{R})$ in 1909. Johann Radon described the reconstruction of a function from its line integral values in his article in 1917. The entry of computers amplified the importance of these transforms in the second half of the past century, because the above named transforms became the theoretical base of algorithms that are used in signal processing or in computer tomography. In such a way they give possibilities to remove noise from the sound or visual recordings, to compress the image data before their transmission, to find the trend in given time series or to identify malignant tumors in a human body.

The outline of this article is as follows. Some basic information about the definition and construction of the Fourier transform together with examples is presented in Section 2. The wavelet transform is described and applied on the given data in Section 3. The Radon transform and its usage in medicine is discussed in Section 4.

2. Fourier transform

For $f \in L^1(\mathbb{R})$, the relation

$$F(\omega) = \int_{-\infty}^{\infty} f(x)e^{2\pi i\omega x} dx, \quad \omega \in \mathbb{R}, \quad (1)$$

represents the continuous Fourier transform (FT) of a function f . The integral transform

$$F^{-1}(x) = \int_{-\infty}^{\infty} F(\omega)e^{-2\pi i\omega x} d\omega, \quad x \in R, \quad (2)$$

is the inverse Fourier transform.

The discrete analogies of the relations (1) and (2) are suitable for computer implementation. If sampled values f_0, \dots, f_{N-1} of a function f are given, the components of the discrete Fourier transform (DFT) are defined by

$$F_k = \sum_{j=0}^{N-1} f_j e^{\frac{2\pi ijk}{N}}, \quad k = 0, \dots, N-1, \quad (3)$$

and the components of the discrete inverse Fourier transform (DIFT)

$$f_j = \frac{1}{N} \sum_{k=0}^{N-1} F_k e^{-\frac{2\pi ijk}{N}}, \quad j = 0, \dots, N-1. \quad (4)$$

The number of operations that are used for calculation of the DFT by relation (3) has the order $O(N^2)$. But there is an effective numerical algorithm of fast Fourier transform (FFT) that allows to reduce the number of used operations. This algorithm is based on the properties of exponential functions and on an ingenious arrangement of computation that is given in the next lemma (see [5]).

Lemma 1 (Danielson-Lanczos, 1942) Let N be even. Then

$$F_k = F_k^0 + W^k F_k^1, \quad k = 0, \dots, N-1, \quad (5)$$

where $F_k^0 = \sum_{j=0}^{\frac{N}{2}-1} W^{jk} f_{2j}$, $F_k^1 = \sum_{j=0}^{\frac{N}{2}-1} W^{jk} f_{2j+1}$, $W = e^{\frac{2\pi i}{N}}$ and $W^{jk} = e^{\frac{2\pi ijk}{N}}$.

Lemma 1 can be applied recurrently M times if $N = 2^M$. The FFT in the following way reduces the order of the number of operations that are necessary to compute the Fourier coefficients from $O(N^2)$ to $O(N \log N)$. Note that the schematic expression of the computation that is generated by relation (5) looks like a butterfly. This is the reason, why the name “butterfly” is used for one loop of the FFT process.

Example 1 The function $f(x) = \sin 1500x$ is impaired by random noise. The DFT for $N = 200$ values is computed and expressed in Figure 2.

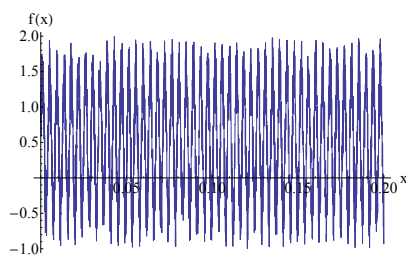


Figure 1: The original signal

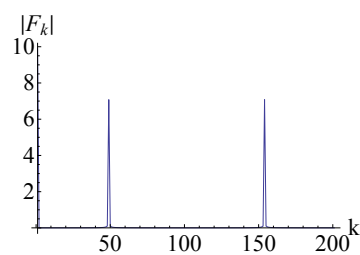


Figure 2: The signal after the FT

The signal is a quantity that depends on one or more variables. For example, a sound is a one dimensional signal that depends on time and a digital photograph is two dimensional signal over a matrix of pixels. While a signal gives information about variability with respect to independent variables, its FT gives information about frequencies that occur in the given signal. The knowledge of the frequency spectrum of a signal is important, because it helps to analyze this signal. The low frequencies are important for identification of the signal. The higher frequencies often represent the noise.

In the signal processing, the DFT is applied on the given data at first. This way the time depending function changes on the frequency depending function. Then, the received Fourier coefficients can be modified according to monitored aims. For instance, the noise can be removed from the given signal if the Fourier coefficients with frequency higher than the given treshold λ are put to zero. A signal is compressed when the majority of Fourier coefficients is neglected. The IDFT is applied on the rest of the Fourier coefficients in the end.

The real part of the FT – the discrete cosine transform (DCT)

$$C_{km} = \sum_{j=0}^{N-1} \sum_{l=0}^{P-1} f_{jl} \cos \frac{2\pi ijk}{N} \cos \frac{2\pi ilm}{P}, \quad k = 0, \dots, N-1, \quad m = 0, \dots, P-1, \quad (6)$$

is the proper tool if some real 2D data are processed. For instance, the DCT is used for compression of an image in the JPEG format.

Example 2 Removing noise from the given data by hard tresholding ($\lambda=0.5$).

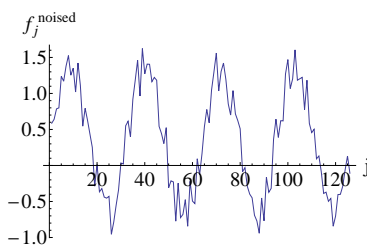


Figure 3: The noised data

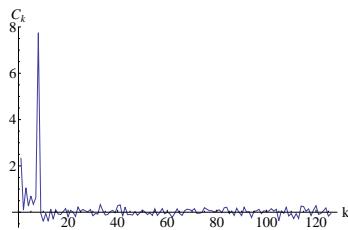


Figure 4: The DCT of the noised data

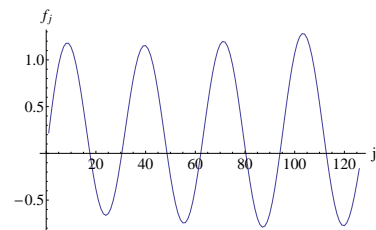


Figure 5: The data with removed noise

When the DFT is applied to data, the information about the frequency is received but the information about the time is lost. It means that the DFT is suitable for an analysis of stationary signals and it does not detect the jump changes and the trends that occur in non-stationary signals. The time localization of the signal can be reached if the short time Fourier transform (STFT) is used. The STFT is defined by

$$F(\omega, t) = \int_{-\infty}^{\infty} f(x) w_r \left(\frac{x-t}{r} \right) e^{-i\omega x} dx, \quad (7)$$

where $w_r(x) = w(\frac{x}{r})$ is a window (a function smooth enough that is compactly supported). The parameter r allows to adjust the length of the analyzed signal segment. The size is the same for all windows in the discrete version of STFT.

3. Wavelet transform

Let f be in $L^2(\mathbb{R})$ and ψ be the wavelet (i.e. a function that can be imagined like a small wave that decreases quickly to 0 in $\pm\infty$). The wavelet transform is defined by

$$W_\psi(a, b) = \frac{1}{|a|} \int_{-\infty}^{\infty} f(x) \psi\left(\frac{x-b}{a}\right) dx. \quad (8)$$

Here a is a scale¹ and b is a translation. If $a \in \mathbb{R}$ and $b \in \mathbb{R}$ we speak about the continuous wavelet transform (CWT).

Example 3 The CWT of the given signal using the Mexican hat wavelet $\psi(x) = \frac{2}{\sqrt{3}}\pi^{-1/4}(1-x^2)e^{-x^2/2}$ is done. The corresponding scalogram (i.e. the graph in which the density of energy $E(a, b) = |(W_\psi f)(a, b)|^2$ for the scale a and for the position b is expressed) is given in Figure 7. Here, large absolute values of the wavelet coefficients are shown darker.

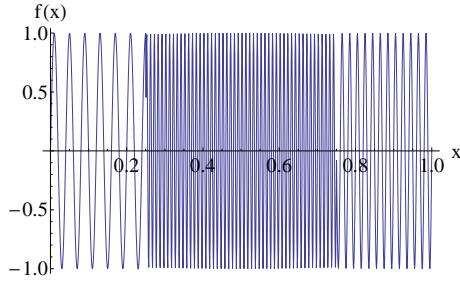


Figure 6: The original signal

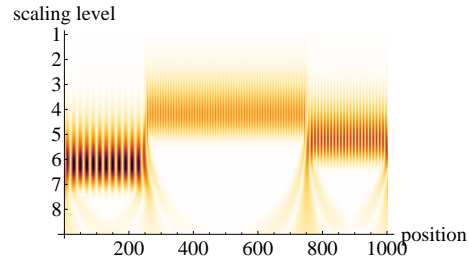


Figure 7: The scalogram

If a and b are discrete values we speak about the discrete wavelet transform (DWT). The dyadic dilatation $a = 2^j$ and the translation $b = k$, where $j, k \in \mathbb{Z}$, are used for the sake of the computation effectivity. The DWT has then the form

$$W_{j,k} = 2^{\frac{j}{2}} \int_{-\infty}^{\infty} f(x) \psi(2^j x - k) dx. \quad (9)$$

The discrete reconstruction is realized by

$$f(x) = \sum_{j \in \mathbb{Z}} \sum_{k \in \mathbb{Z}} 2^{\frac{j}{2}} W_{j,k} \psi(2^j x - k). \quad (10)$$

But the system $2^{\frac{j}{2}} \psi(2^j x - k)$ does not need to be orthonormal for general functions ψ . One of possibilities how to receive an orthonormal basis in $L^2(\mathbb{R})$ is to use the multiresolution analysis (MRA)², where the spaces $V_j \subset L^2(\mathbb{R})$ ($j \in \mathbb{Z}$) that satisfy

$$V_j \subset V_{j+1}; \quad \bigcap_{j \in \mathbb{Z}} V_j = \{0\}; \quad \bigcup_{j \in \mathbb{Z}} V_j = L^2(\mathbb{R});$$

¹Scales and the frequencies are connected: Higher scales correspond to lower frequencies.

²The construction of wavelets by means of the MRA based on the existence of a scale function φ was proposed by Mallat in 1988.

$\exists \varphi \in V_0 : \{\varphi(x - k)\}_{k \in \mathbb{Z}}$ is a complete orthogonal set in $L^2(\mathbb{R})$;

$$f \in V_0 \Leftrightarrow f(2^j x) \in V_j$$

are constructed.

It follows from the properties of the spaces V_j given above that there exist the subspaces W_j orthogonal to V_j such that $V_{j+1} = V_j \oplus W_j$.

If $\{V_j\}$ is the MRA and φ is the scaling function that satisfies the dilatation equation

$$\varphi(x) = \sqrt{2} \sum_{k \in \mathbb{Z}} u_k \varphi(2x - k), \quad (11)$$

then

$$\psi(x) = \sqrt{2} \sum_{k \in \mathbb{Z}} v_k \varphi(2x - k), \text{ where } v_k = (-1)^{k-1} \overline{u_{1-k}} \quad (12)$$

is the associated wavelet correspondig to the MRA.

The spaces V_j resp. W_j are generated by functions that are dilatations and translations of the scaling function and the associated wavelet function³

$$V_j = \text{span}\{\varphi_{j,k}\}_{j,k \in \mathbb{Z}}, \text{ where } \varphi_{j,k}(x) = 2^{j/2} \varphi(2^j x - k), \quad (13)$$

$$W_j = \text{span}\{\psi_{j,k}\}_{j,k \in \mathbb{Z}}, \text{ where } \psi_{j,k}(x) = 2^{j/2} \psi(2^j x - k). \quad (14)$$

The space V_{j+1} can be interpreted as an approximation space in $L^2(\mathbb{R})$ and $V_{j+1} = V_0 \oplus W_0 \oplus W_1 \oplus \dots \oplus W_j$. It means that every function $f \in L^2(\mathbb{R})$ can be written as

$$f(x) = \sum_{k \in \mathbb{Z}} a_{0,k} \varphi_{0,k}(x) + \sum_{j \geq 0} \sum_{k \in \mathbb{Z}} b_{j,k} \psi_{j,k}(x), \quad (15)$$

where $a_{0,k}$ are the scaling coefficients and $b_{j,k}$ are the wavelet coefficients of f on the level j .

Let $\langle f, g \rangle$ be the inner product in $L^2(\mathbb{R})$. In what follow, we will denote the vectors of wavelet coefficients of f on the level j by

$$\mathbf{b}_j = (b_{j,k})_{k \in \mathbb{Z}}, \text{ where } b_{j,k} = \langle f, \psi_{j,k} \rangle, \quad (16)$$

and the vectors of scaling coefficients of f on the level j as

$$\mathbf{a}_j = (a_{j,k})_{k \in \mathbb{Z}}, \text{ where } a_{j,k} = \langle f, \varphi_{j,k} \rangle. \quad (17)$$

Computation of wavelet coefficients is divided in two parts in the Mallat algorithm (see [3]).

³Note that multivariable wavelets are constructed in the form of the tensor product. For instance, a 2D MRA on the first level can be constructed from a decomposition

$$V_1^1 \oplus V_1^2 = (V_0^1 \otimes V_0^2) \oplus (V_0^1 \otimes W_0^2) \oplus (W_0^1 \otimes V_0^2) \oplus (W_0^1 \otimes W_0^2)$$

and the wavelet basis is given by $\{\varphi_{0,k} \otimes \varphi_{0,l}\}_{l \in \mathbb{Z}} \cup \{\varphi_{0,k} \otimes \psi_{0,l}, \psi_{0,k} \otimes \varphi_{0,l}, \psi_{0,k} \otimes \psi_{0,l}\}_{l \in \mathbb{Z}}$.

In the first one – decompositon, the wavelet coefficients are computed from the given data: The vector \mathbf{a}_m of the scaling coefficients of function f is given for $m \in Z$ large enough. The wavelet transform $\mathbf{b}_{m-1}, \dots, \mathbf{b}_{m-l}, \mathbf{a}_{m-l}$ of f is computed for a chosen $l \in N$ in the following way:

$$\mathbf{b}_j = D(\mathbf{a}_{j+1} * \tilde{\mathbf{v}}), \quad \mathbf{a}_j = D(\mathbf{a}_{j+1} * \tilde{\mathbf{u}}), \quad j = m - 1, \dots, m - l, \quad (18)$$

where $D(z_n) = z_{2n}$ is the downsampling operator, $\tilde{z}_n = \overline{z_{-n}}$ is the operator of conjugated reflexion and $\mathbf{b}_{j+1} * \tilde{\mathbf{u}}$ is the convolution of the vector \mathbf{b}_{j+1} with the vector $\tilde{\mathbf{u}}$.

In the second part – reconstruction, the vector \mathbf{a}_m is constructed from the received set $\mathbf{b}_{m-1}, \dots, \mathbf{b}_{m-l}, \mathbf{a}_{m-l}$ in the following way:

$$\mathbf{a}_{j+1} = (U(\mathbf{a}_j)) * \mathbf{u} + (U(\mathbf{b}_j)) * \mathbf{v}, \quad j = m - l, \dots, m - 1, \quad (19)$$

where $U(z_n) = z_{n/2}$ for n even and zero while for n odd it is the operator of upsampling.

This process is realized by using proper quadratic mirror filters in signal processing. The given vector of values that represents a signal goes through the lowpass filter and highpass filter in the first phases of computation. The approximation coefficients a_j and detail coefficients b_j are received. Note that the approximation coefficients belong to low frequencies that represent trends and the details belong to high frequencies that can be interpreted as noise. The received outputs are downsampled and they can be filtered again. It is possible to express this process graphically in the form of the completing wavelet tree. In the second phasis the received approximation and details are upsampled and then they are filtered by conjugate filters.

Before reconstruction it is possible to modify the wavelet coefficients. For example, noise is removed from the given signal, if the wavelet coefficients $b_{i,j}$ that have smaller frequency than the chosen treshold λ are set to zero. Also the soft thresholding with the modified coefficients $\tilde{b}_{j,k} = \begin{cases} 0 & \text{if } b_{j,k} < \lambda, \\ \text{sgn } b_{j,k} |b_{j,k} - \lambda| & \text{in other cases} \end{cases}$ can be used.

Example 4 Removing noise from the given data by means of the wavelet transform. Here, the Daubechies wavelet Db4 was used.

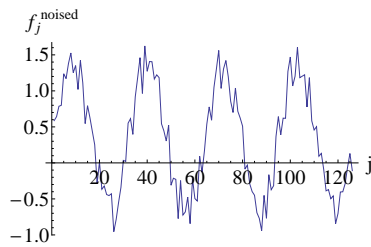


Figure 8: The noised data

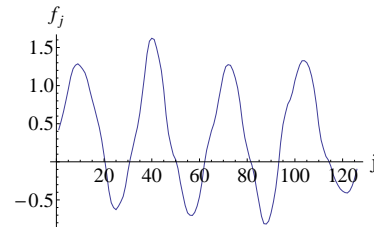


Figure 9: The data with removed noise

If a 2D visual signal has to be compressed, it is decomposed into horizontal, vertical, diagonal and approximation coefficients in the beginning. Only the approximation coefficients are used for the next decomposition, because only they hold the important information. The received details are cut on asked level. The DWT with the hard thresholding is used in the JPEG2000 format.

Example 5 The wavelet transform of the given image.



Figure 10: The original image



Figure 11: The decomposition of the image up to refinement level 2

4. Radon transform

Generally, the Radon transform⁴ of a function f from the Schwartz space $S(R^n)$ is the integral transform

$$g(t, \theta) = \int_{x \cdot \theta = t} f(x) dm(x), \quad (20)$$

where $\{x \in R^n : x \cdot \theta = t\}$ is a hyperplane for a fixed $t \in R$ and $\theta \in S^{n-1}$, $S^{n-1} = \{x \in R^n : \|x\| = 1\}$ is a sphere, and dm is the Lebesgue measure.

At the beginning of the last century, the Austrian mathematician J. F. Radon found the way how to reconstruct the function f from the values g . If $n = 3$ the inverse Radon transform has the form

$$f(x) = -\frac{1}{8\pi^2} \Delta_x \int_{S^3} g(\langle x, \theta \rangle, \theta) dS_\theta^3 \quad (21)$$

and if $n = 2$ the inverse Radon transform (IRT) is

$$f(x) = \frac{1}{4\pi^2} \int_{S^2} \text{v.p.} \int_{-\infty}^{\infty} \frac{g'_t(t, \theta)}{x \cdot \theta - t} dt dS_\theta^2, \quad (22)$$

⁴Note that the Radon transform is closely connected to the Fourier transform. The n D Fourier transform of f is the composition of the Radon transform of f and 1D Fourier transform.

where “v.p.” means “within the meaning of the Cauchy principal value”. The Radon transform (RT) of a function $f \in L^2(R^2)$ is given by the line integral

$$g(t, \varphi) = \int_{\langle x, \theta \rangle = t} f(x) dx, \quad \theta = (\cos \varphi, \sin \varphi)^T. \quad (23)$$

The inverse Radon transform (IRT) by

$$f(x) = \frac{1}{4\pi^2} \int_0^{2\pi} \text{v.p.} \int_{-\infty}^{\infty} \frac{g'_t(t, \varphi)}{x \cdot \theta - t} dt d\varphi. \quad (24)$$

The relations (23) and (24) became the theoretical basis of the computer tomography with the following basic idea: If a body is irradiated by X-rays or other type of waves, the intensity of the radiation I changes depending on the density distribution f of substances through which it passes. When the the initial intensity of radiation is I_0 and $l(x, \theta)$ is a line which the ray goes along, this change can be expressed as

$$\ln \frac{I_0}{I} = \int_{l(x, \theta)} f(x) dx. \quad (25)$$

It means that the value $\ln \frac{I_0}{I}$ is equal to the Radon transform of f . When measurements for different directions of rays are realized, the inverse Radon transform can be used to determine the density distribution f in the studied plane.

The received results can be demonstrated graphically. The measured values for each ray are represented by the corresponding gray's shade. This allows to express graphically the density of distribution in the planar section. The space image arises by composition of the images from different planar sections.

Example 6 The Radon transform in R^2 of the given picture is done. Its graphical expression – sinogram – is given in Figure 13. Here, lighter color is assigned to higher values of the RT.

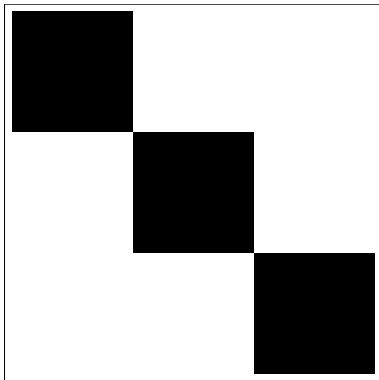


Figure 12: The original image

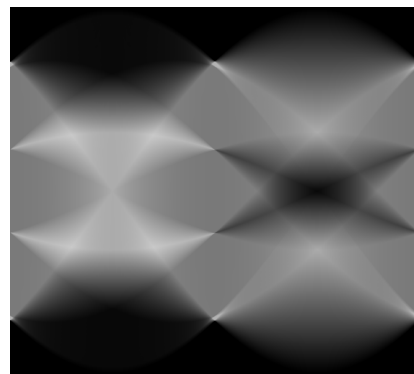


Figure 13: The sinogram

In practice, all measurements and evaluation are realized on the tomograph that consists of a scanner, computer and monitor. A program for the evaluation of the data provided by scanner is built in the computer. This program is based on a numerical algorithm. There are three basic types of algorithms in computer tomography that are used for reconstruction – convolution algorithms, algebraic algorithms and Fourier reconstruction. We focus only on one of the convolution algorithms that is used in medicine.

The formula (24) for inverse Radon transform is the base for the convolution reconstruction algorithms in the plane. But the form of algorithm depends on the design of the scanner (the formulas for parallel-ray geometry and divergent-ray geometry see [5]). Recent tomographic scanners are equipped with the 4th generation of detectors placed around the circumference of a circle that moves along the source sending divergent rays.

Denote

D – the distance of the source from the origin of the coordinate system,

L – the distance of the reconstructed point (ρ, ψ) from the source,

β – the angular position of the source,

γ – the angle that gives the location of a ray within a fan,

γ' – the angle of the ray that passes through the reconstructed point (ρ, ψ) (see Figure 14).

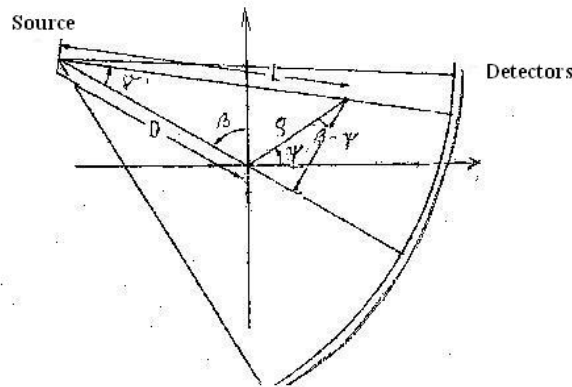


Figure 14: Measurement of data

The formula for the inverse Radon transform is converted into the form

$$f(\rho, \psi) = \frac{D}{2} \int_0^{2\pi} \int_{-\infty}^{\infty} v(L \sin(\gamma' - \gamma)) g(\beta, \gamma) \cos \gamma d\gamma d\beta. \quad (26)$$

The derivation can be found in [2].

If the source is rotated p times about the same angle $\Delta\beta = \frac{2\pi}{p}$ and it always sends $2q$ rays that form an equal angle $\Delta\gamma = \frac{\pi}{2q}$, the values $g(\beta_j, \gamma_l)$ are received.

Now, the integral in equation (26) can be calculated by the trapezoidal rule

$$f(\rho, \psi) \sim \frac{D}{2} \Delta\beta \Delta\gamma \sum_{j=0}^{p-1} \sum_{l=-q}^q v(L \sin(\gamma_k - \gamma_l)) g(\beta_j, \gamma_l) \cos \gamma_l. \quad (27)$$

The reconstruction of the function f is divided into two phases. First, the convolution of functions v and g (i.e. the sum inside the formula (27)) is calculated and, second, the back projection is performed.

5. Conclusion

The Fourier transform and the wavelet transform are used in signal processing, they allow to extract information from many different kinds of data, they can help to analyze voice or to compress pictures, they can also serve to analyze variability, to remove noise or to detect significant moments in the time series that are used in economy.

Also the tomographic methods have broad application. We can meet them not only in medical diagnostics, but they are also used in studying structure of materials (the study of composite materials), in prospecting (mapping oil deposits, the ocean floor), in pyrometry (temperature in the blast furnace) or in astronomy.

References

- [1] Jelínek, J., Segeth, K., Overton, T.R.: Three-dimensional reconstruction from projections. *Apl. Mat.* **30** (1985), 92–109.
- [2] Kak, A. C., Slaney, M.: *Principles of computerized tomographic imaging*. Society of Industrial and Applied Mathematics, IEEE Press New York 1988.
- [3] Najzar, K.: *Základy teorie waveletů*, 1. vyd. Praha: Karolinum, 2004, 198 s. Učební texty Univerzity Karlovy v Praze.
- [4] Radon, J.: *Über die Bestimmung von Functionen durch ihre Integralwertelangs-gewisser Mannigfaltigkeiten*. *Berichte Sachsische Academie der Wissenschaften*, 1917.
- [5] Segeth, K.: *Numerický software I*. Karolinum, Praha, 1998.